Forest Ecology and Management 302 (2013) 308–318

Contents lists available at SciVerse ScienceDirect

Forest Ecology and Management

journal homepage: www.elsevier.com/locate/foreco

Multi-temporal analysis reveals that predictors of mountain pine beetle infestation change during outbreak cycles

Jonathan A. Walter *, Rutherford V. Platt

Department of Environmental Studies, Gettysburg College, Gettysburg, PA 17325, USA

ARTICLE INFO

Article history:
Received 24 January 2013
Received in revised form 23 March 2013
Accepted 25 March 2013
Available online 27 April 2013

Keywords:
Mountain pine beetle
Outbreak
Red attack
Remote sensing
Time series

ABSTRACT

Over the past two decades, severe mountain pine beetle (MPB) outbreaks have affected several million hectares of forest in western North America. The extensive ecological and economic damage caused by widespread insect infestations make understanding the development and spread of MPB outbreaks critical. This study uses a time series of Landsat5 TM and Landsat7 ETM + images to map the spread of mortality due to MPB infestation in Arapaho–Roosevelt National Forest, Colorado, between 2003 and 2010. The Normalized Difference Vegetation Index (NDVI) and change in the Normalized Difference Moisture Index (NDMI) were used to classify red attack and non-red attack stands based on a maximum likelihood algorithm with manually selected training classes. The classification was validated by comparison with independent interpretations of aerial photography and high-resolution satellite imagery. The classification had good agreement (84.5–90.5% total accuracy). Cluster analysis for time series showed infestations originating in several different locations on the landscape early in the time series and subsequent infestations likely represent a combination of dispersal from outbreak populations and independent population growth. Analysis using conditional inference trees suggested that a combination of forest composition, topography, and dispersal predicted the distribution of MPB infestation on the landscape and that the importance of these variables changed as the outbreak developed. In early years, red attack was associated with forest and topographic characteristics known to influence susceptibility to MPB. Over time, beetle pressure became an increasingly important predictor of red attack, but in later years host tree availability played an important role in outbreak spread. If this pattern occurs consistently in MPB outbreaks, knowledge of these patterns could aid managers in targeting their efforts to reduce damage resulting from MPB outbreaks.

1. Introduction

Since the 1990s, outbreaks of mountain pine beetle (*Dendroctonus ponderosae* Hopkins) have killed over 9 million hectares of forest in Canada (Westfall, 2007) and approximately 1.5 million hectares in the USA (USDA Forest Service, 2012). Although endemic to western North America, recent outbreaks are particularly severe, and this high severity has been linked to climate change (Carroll et al., 2004) and disturbance suppression (Taylor and Carroll, 2004). Mountain pine beetle (hereafter, MPB) outbreaks are significant forest disturbances that affect wildlife, watershed quality, and recreational use in addition to causing extensive timber losses (Safranyik et al., 1974; Sims et al., 2010). Several studies have also linked changes in fuel quantity, moisture, and arrangement caused by MPB mortality to changes in wildfire risk and fire behavior (Jenkins et al., 2008, 2012; Klutsch et al., 2011; Simard et al., 2011; Jolly et al., 2012; Schoennagel et al., 2012). Because of these dramatic effects, ecologists and forest managers require an understanding of the mechanisms that drive MPB outbreaks to predict and mitigate future outbreaks.

Native to western North America, MPB can reproduce within most pine species in its range, though lodgepole pine (*Pinus contorta* var. *latifolia* Engelm.) is considered its primary host and ponderosa pine (*Pinus ponderosae*) and sugar pine (*Pinus lambertiana*) are also major hosts (Safranyik and Carroll, 2006). Trees that have been infested by MPB are conspicuous because of changes to their foliage; approximately 6–8 months after infestation, the crowns of infested trees begin to turn from green to yellow to red due to moisture loss and degradation of pigments, with the shift from green to red completing in late summer ≈12 months after the tree was first attacked (Safranyik and Carroll, 2006). In subsequent years, dead foliage drops from the tree (Goodwin et al., 2008). These stages are referred to as red-attack and grey-attack, respectively. The spectral changes to the forest canopy during the red attack and grey attack stages of MPB infestation have been detected

* Corresponding author. Present address: Department of Environmental Sciences, Univers of Virginia, P.O. Box 400123, Charlottesville, VA 22904, USA. Tel.: +1 434 924 0958.
E-mail address: jaw3es@virginia.edu (J.A. Walter).

0378-1127/$ - see front matter © 2013 Elsevier B.V. All rights reserved.
http://dx.doi.org/10.1016/j.foreco.2013.03.038

with high accuracy using satellite and airborne remote sensing (Coops et al., 2006; Wulder et al., 2006a; Goodwin et al., 2008; Meddens et al., 2011). Delineating outbreak areas using remotely sensed imagery can offer improvements in accuracy over aerial detection surveys while providing continuous, large-area estimates of tree mortality that are difficult or impossible to obtain using a ground-based survey (Wulder et al., 2006b). Consequently, maps of MPB outbreak derived from remotely sensed imagery have been used to characterize susceptibility to MPB infestation (Coops et al., 2006; Wulder et al., 2006a) and to examine spatiotemporal patterns of outbreak development (Goodwin et al., 2008). Results from such studies indicate that red attack can be predicted using characteristics such as elevation, direct solar radiation, and forest age, density, and species composition (Coops et al., 2006; Wulder et al., 2006a).

In this system, favorable forest characteristics including size, age, density, and species composition, are understood to set the stage for outbreaks that are triggered by climate and weather (Safranyik and Carroll, 2006). However, much of what is known about susceptibility to MPB infestation describes how likely a tree or stand is to become infested if an outbreak occurs. At the landscape scale, an average outbreak cycle lasts around 10 years (Safranyik and Carroll, 2006), during which period the stands making up a landscape may exhibit predictable spatiotemporal patterns in outbreak development and spread. Thus, a related but less-studied line of inquiry focuses on understanding the spatiotemporal dynamics of MPB infestation as it spreads over a landscape during an outbreak cycle. One approach builds on the concept of susceptibility to MPB infestation by also taking into account the severity and proximity of current MPB infestations to define a risk rating for MPB (Shore and Safranyik, 1992). This strategy yields predictions of MPB infestation with greater spatial and temporal specificity than susceptibility rating (Shore et al., 2000), but if the environmental characteristics of infested areas tend to change from the beginning of an outbreak cycle through the outbreak crash, an understanding of those dynamics could improve predictions of outbreak spread and be incorporated into a framework that targets stands for management.

In this study, we explore MPB activity in Arapaho and Roosevelt National Forests from 2003 to 2010. First, we examine spatiotemporal characteristics of the spread of the infestation by detecting recent MPB outbreak in a time series of Landsat 5TM and Landsat7 ETM+ (pre scan-line corrector failure) satellite imagery and using cluster analysis methods for time series to examine the spatiotemporal structure of the outbreak. Second, we assess how topography, forest structure, and beetle pressure affected the development and spread of this infestation using conditional inference trees. By employing a multi-temporal approach we offer a unique investigation into patterns of outbreak development and environmental predictors on outbreak spread. We hypothesize that the occurrence of MPB infestation will be most strongly related to topography and stand structure during initial outbreak stages when populations are rising to epidemic levels. As the outbreak reaches its peak, we hypothesize that dispersal and pressure from nearby outbreaking populations will increase in importance, but that the predictive power of all variables will decline between the peak of the outbreak and its crash.

2. Methods

2.1. Study area

Arapaho and Roosevelt National Forests (ARNF) are located in north-central Colorado, USA, covering approximately 7000 km^2 between Boulder, CO, and the Wyoming state boundary (Fig. 1). Roughly 5300 km^2 are forested. Average daily minimum and maximum temperatures are −6.6 °C and 11.6 °C, respectively, and mean annual precipitation is 48.4 cm (1907–2011 averages, Western Regional Climate Center, Grand Lake 1 NW station, latitude: 40.267, longitude: −105.832, elevation: 2650 m, http://www.wrcc.dri.edu; accessed 5 February 2012). Elevation in the study area ranges from ≈1700–4300 m leading to a diversity of forest communities. Two major hosts of MPB, lodgepole pine (*Pinus contorta*) and ponderosa pine (*Pinus ponderosa*) are abundant in ARNF. Ponderosa pine dominates dry, low-elevation sites, with Lodgepole pine and Douglas-fir (*Pseudotsuga menziesii*) becoming more abundant >2500 m (Marr, 1961; Peet, 1981). The importance of limber pine (*Pinus flexilis*) and aspen (*Populus tremuloides*) also increases with elevation (Marr, 1961). At high elevations, forests are dominated by Engelmann spruce (*Picea engelmanni*), subalpine fir (*Abies lasiocarpa*) and limber pine (*Pinus flexilis*). Above ≈3500 m, forests begin to be replaced by alpine tundra (Peet, 1981).

2.1.1. Remote sensing of red attack

MPB red attack was detected using a time series of six Landsat 5 TM and Landsat 7 ETM+ images spanning 2002–2010, dated 10 August 2002, 22 September 2003, 11 September 2005, 26 August 2006, 21 August 2009, and 24 September 2010. All Landsat scenes are from path 32 row 34 and were obtained with radiometric and geometric corrections (Level 1T) applied, and the Landsat 7 scene (10 August 2002) was taken prior to failure of the scan line corrector in May 2003. Selected images had low cloud cover (<10% of study area). Images with late summer dates were selected because of the ≈12 month lag between infestation and completing the shift to the red attack stage. This convention is followed by several studies (Coops et al., 2006; Wulder et al., 2006a; Goodwin et al., 2008; Meddens et al., 2011). Where gaps in the time series occur (intervals between images ⩾2 years) no images fitting our selection criteria were available.

All images were pre-processed by converting to exoatmospheric reflectance, performing dark object subtraction, and clipping the image to represent only forested areas of Arapaho–Roosevelt National forest as defined by the USFS R2Veg geodatabase (USDA Forest Service, 2009). Reflectance (r_p) was calculated using the equation:

$$r_p = \frac{L_\lambda \times d^2}{\mathrm{ESUN}_\lambda \times \cos q_s}, \quad (1)$$

where L_λ is the spectral radiance, d is the Earth–Sun distance in astronomical units, $ESUN_\lambda$ is the mean solar exoatmospheric irradiance, and q_s is the solar zenith angle in degrees. $ESUN_\lambda$ values for Landsat 5 images were obtained from Chander and Markham (2003) and from the *Landsat 7 Data Users Handbook* (2007). Spectral radiance (L_λ) was calculated as:

$$L_\lambda = LMIN_l + \frac{LMAX_\lambda - LMIN_\lambda}{QCALMAX - QCALMIN} \times QCAL - QCALMIN, \quad (2)$$

where $QCAL$ is the calibrated and quantized scaled radiance in units of digital numbers (DNs), $LMIN_l$ is the spectral radiance at $QCAL = 0$, $LMAX_\lambda$ and $LMIN_\lambda$ are the spectral radiance at $QCAL = QCALMAX$ and $QCAL = QCALMIN$, respectively, from Chander et al. (2009).

Cloud cover was manually removed such that an area obscured by cloud in 1 year was removed from all images. This area totaled ≈295 km^2, <6% of the study area.

The Normalized Difference Vegetation Index [(TM4 − TM3)/(TM4 + TM3)] and Normalized Difference Moisture Index [(TM4 − TM5)/(TM4 + TM5)] transformations were applied to all images. The Normalized Difference Moisture Index (NDMI) is similar to the Normalized Difference Vegetation Index (NDVI),

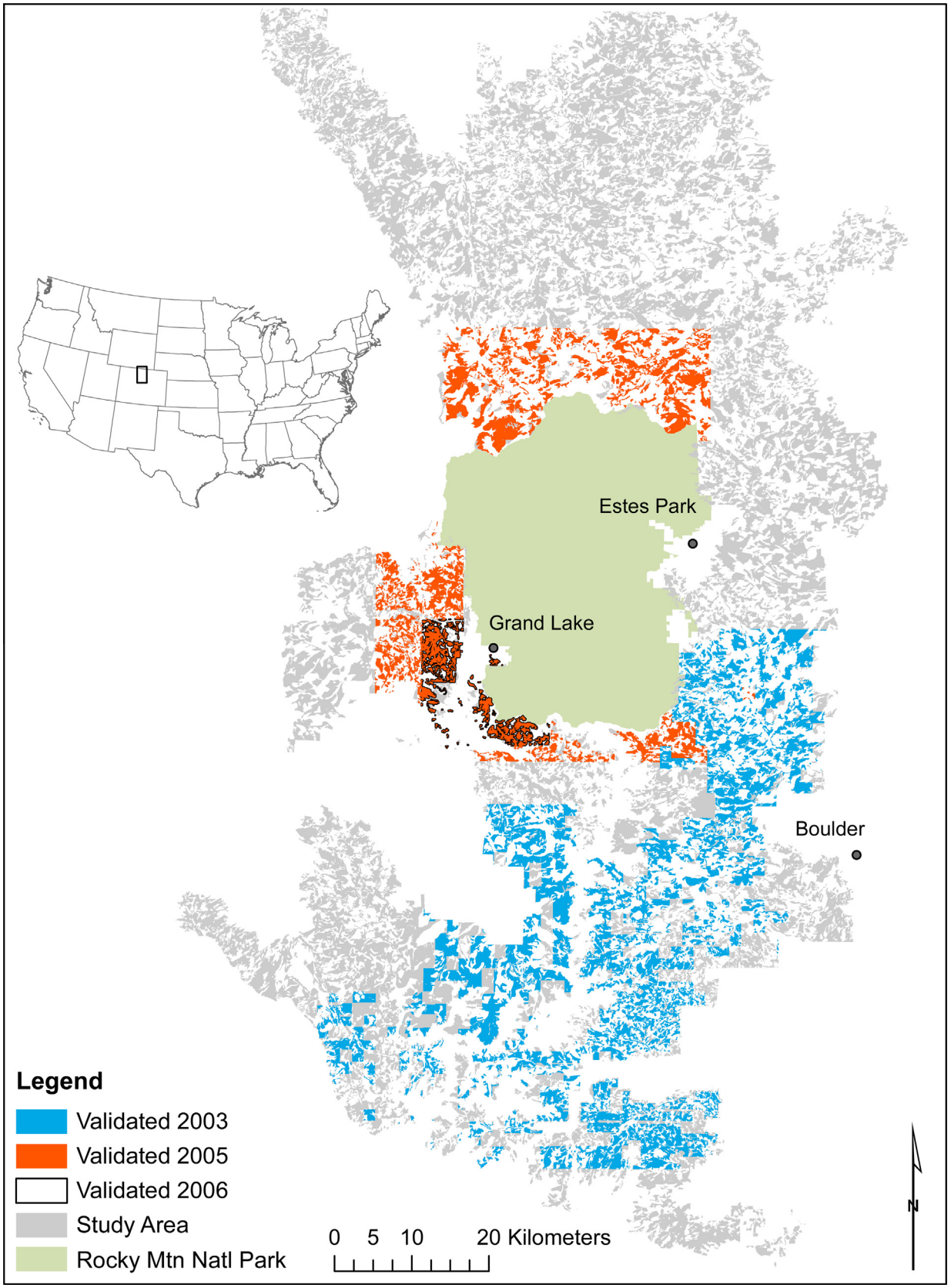

Fig. 1. Site map. The study area (grey) represents forested areas in ARNF, after cloud cover (<6% of study area) has been removed.

but instead of sensing the "red edge" created by the low reflectance of vegetation in Landsat TM3 (red) and high reflectance in TM4 (near-infrared), NDMI is sensitive to moisture levels by combining the near-infrared (TM4) and mid-infrared (TM5) bands (Jin and Sader, 2005). Image differencing of the NDMI band was used to create a band measuring change in NDMI between

consecutive images, representing canopy moisture loss due to MPB infestation (Goodwin et al., 2008).

Red attack was detected using a supervised maximum likelihood classification performed on the combination of initial NDVI and change in NDMI. For example, Red Attack in 2005 was detected using a composite of 2003 NDVI and change in NDMI from 2003 to 2005. Thus, red attack was detected in 5 years: 2003, 2005, 2006, 2009, and 2010. Two classes, "Red Attack" and "Non Red Attack", were assigned using a manually selected training sample of each class. Training samples were created based on visual interpretation of a color-infrared composite image, initial NDVI value, and change in NDMI, and separate training samples were selected for each time step. Subsequently, the training samples were checked against Forest Service Aerial Detection Survey data (USDA Forest Service, 2013) to confirm that they represented the appropriate class. Areas exhibiting red attack were expected to have high initial NDVI, representing healthy forest, and show a decrease in NDMI between images due to MPB mortality. The non-red-attack training sample included areas with a variety of NDVI values and approximately stable or increasing NDMI.

In general, current best practices for analyzing time series of satellite imagery include normalizing reflectance in all images to a reference image, but this was not necessary in our study. We selected different training classes at each time step, which should account for spectral differences between images and the use of ratio-based indices like NDVI and NDMI should also minimize differences between images. Although we do use image differencing (change in NDMI), Song et al. (2001) indicate that classifications based on image differencing, even using images that have not been converted to reflectance and atmospherically corrected, will not lead to classification error if the classification algorithm does not assume no change in any class. Thus, the reflectance conversions and atmospheric corrections we performed should have no substantial impact on the accuracy with which red attack was detected.

It is important to note that this study detected change in red attack status, but because of the time lag between the infestation of a tree and its crown shifting to red and the time elapsed between images, we detected the results of infestation that occurred at least 1 year previous. Additionally, it is possible that other biotic or abiotic agents cause some detected tree mortality; however MPB outbreak is known to have caused significant damage in ARNF during the study period (Meddens et al., 2011; USDA Forest Service, 2012). We performed image processing and classification steps using ENVI version 4.8 (Exelis Visual Information Solutions, Boulder, Colorado).

2.1.2. Validation

The classified images for 2003 and 2005 were validated by comparison with high-resolution aerial photography (1 m resolution) at 200 randomly placed points. Aerial photography has previously been shown to accurately estimate MPB-caused mortality (Dillman and White, 1982; Klein, 1982). Each validation point was assigned to the Red Attack or Non-Red Attack class by visual interpretation of the high-resolution image, where a point was considered Red Attack if the majority of trees within a 5 m radius of the point showed signs of red attack. Due to constraints on data availability, different spatial subsets of the study area were evaluated at different times (Fig. 1). Where imagery was available, each classification was validated using aerial photography (USGS digital orthophoto quadrangles, 1 m resolution) taken during late summer of the same year (2005; images taken August 2005) or spring of the following year (2003; images taken April 2004). For 2006, we validated our classification against a QuickBird scene dated 3 September 2006 in Google Earth using the same methodology. The 2009 classification was not validated due to a lack of available high-resolution imagery.

The performance of our classification method was assessed based on overall accuracy (percent correct), quantity disagreement, and allocation disagreement rather than a kappa index (Pontius and Millones, 2011). Quantity disagreement describes the error that results from assigning the incorrect number of pixels to each class, and allocation disagreement describes the error that results from assigning those classes to the wrong location. This is thought to be an improvement over traditional error assessment because kappa indices have been shown to be redundant, difficult to interpret, and potentially misleading (Pontius and Millones, 2011). It is also worth noting that, while previous research has used aerial photography to map MPB red attack with high accuracy (Dillman and White, 1982), interpreting aerial photography is somewhat more subjective than ground-truth observations. We have attempted to preclude the possibility of a biased validation by interpreting the aerial photography blind to the results of the remote sensing classification.

2.2. Outbreak spatiotemporal development

Cluster analysis techniques for times series data can be used to make inferences about what processes drive spatial patterns of insect population dynamics (Liebhold and Elkinton, 1989; Williams and Liebhold, 2000; Aukema et al., 2006). Given a set of locations, each of which has an associated time series, each location is assigned to one of k clusters that maximize the similarity of the time series of the points contained in each cluster. Clusters are then mapped back onto the landscape and to reveal spatial patterns. For example, a bulls-eye pattern indicates that the outbreak originated from a point source and spread outward, while a checkerboard pattern is indicative of multiple simultaneous origins (Aukema et al., 2006).

Because cluster analysis works more effectively on continuous than binary variables, grids cells were aggregated into 25-by-25, 49-by-49, and 99-by-99 blocks and percent red attack (by area) was calculated for each block (Liebhold and Elkinton, 1989). Using three block sizes allowed us to examine the importance of scale in describing time series patterns (Williams and Liebhold, 2000). We excluded grid cells where red attack was not recorded in any year of the time series and applied the k-means non-hierarchical clustering method with $k = 3$ clusters (MacQueen, 1967). The optimal value of k was determined by finding the "elbow" of stress plot using 1–10 clusters (Liebhold and Elkinton, 1989). Cluster analysis was implemented using MATLAB release 2011b (The MathWorks Inc., Natick, Massachusetts).

2.3. Conditional inference tree analysis

We used conditional inference trees to assess whether the spread of the MPB infestation at ARNF is related to topography, forest structure, and spatial variables. Conditional inference trees (CI trees) are similar to classification trees (CARTs) in that they explain variation of a response variable by repeatedly partitioning the data into increasingly homogenous groups using splits based on explanatory variables (De'ath and Fabricius, 2000; Hothorn et al., 2006). The CI tree method implements a permutation test approach that allows it to correct for two problems associated with CARTs, overfitting and a bias toward selecting independent variables with a large number of possible splits (Hothorn et al., 2006; Strobl et al., 2009). Rather than requiring post hoc pruning to prevent overfitting, splits are based on a hypothesis test that the split improves model predictions of the dependent variable (Hothorn et al., 2006).

We constructed a CI tree for each time step in our change detection starting with a dataset of 2000 randomly selected points, with

red attack as a binary response variable. While it is possible for a pixel to be in the red attack class for more than one time step because of mixed pixels, we excluded points from the CI trees after the first year they were classified as red attack. Hence, our models describe how combinations of environmental conditions influenced the likelihood of a new infestation arising through local population growth or spread from an extant outbreak. In 2010, only 6 out of 934 points represented spread of red attack, so a CI model was not built for that time step.

We used following predictor variables to examine environmental characteristics influencing spread of MPB infestation: elevation, aspect (binned into 8 classes: N, NE, E, SE, S, SW, W, NW), percent forest cover, percent lodgepole pine cover, percent ponderosa pine cover, tree size class (based on diameter at root collar (DRC) or diameter at breast height (DBH); established: <2.5 cm DRC, small: 2.5–12.5 cm DBH, medium: 12.5–22.5 cm DBH, large: 22.5–40.5 cm DBH, very large: >40.5 cm DBH). In 2005 and beyond, two additional variables were added to the model: the area of and Euclidian distance from the nearest area infested by MPB (pixel(s) classified as RA) in the previous time step. These variables served as proxies for the size of the MPB population and ease with which MPB could disperse to that location. Because these variables were based on change detection performed by this study, we were unable to compute them for the first time step (2003). Spatial variables were calculated in ArcGIS version 10.0 (ESRI, Redlands, CA), and environmental variables were obtained from the R2Veg database, a continuously updated forest inventory dataset for the US Forest Service Rocky Mountain region (USDA Forest Service, 2009).

The importance of each variable to the model was assessed using random forests, an extension of conditional inference trees. In this procedure, the predictive strength of each variable is assessed based on the performance of trees built using a permutation of random subsets of available predictor variables (Strobl et al., 2009). A covariate that is found to be a significant predictor by random forests may not appear in the best CI tree if a split made by that covariate is equivalent to a split made using another (i.e. a surrogate split), or if other combinations of covariates produce better predictions. By convention, the number of randomly selected predictor variables per tree $\approx\sqrt{n}$, where n is the total number of predictor variables (Strobl et al., 2009). In 2003, $n = 6$ and $n = 8$ for 2005, 2006, and 2009, so random forests were constructed using 2 predictor variables per tree. Variable importance values converged within 18,000 iterations. CI trees and random forests were implemented using the 'party' (Strobl et al., 2008) package in R (R Core Team, 2012).

Receiver-Operator curves (ROCs) were used to evaluate the performance of our CI trees. The accuracy of probability-based prediction models can be assessed in terms of sensitivity (i.e., true positive rate) and specificity (i.e., true negative rate). ROC curves plot the relationship between sensitivity and 1-speficity (i.e., false positive rate) for varying probability thresholds. The area under the ROC curve (AUC) is taken as an index of overall model accuracy. The value of the AUC varies between 0 and 1, with 0.5 representing a model that is no better than random chance and 1 representing a model with a perfect ability to distinguish between two classes (Fielding and Bell, 1997). We used a split-sample approach where 80% of the dataset in each year was randomly selected for model training and the remaining observations were used for validation. The validation samples were used to create ROC curves and to calculate misclassification rates for the CI trees. ROC curves were implemented using the 'ROCR' package (Sing et al., 2005) in R (R Core Team, 2012).

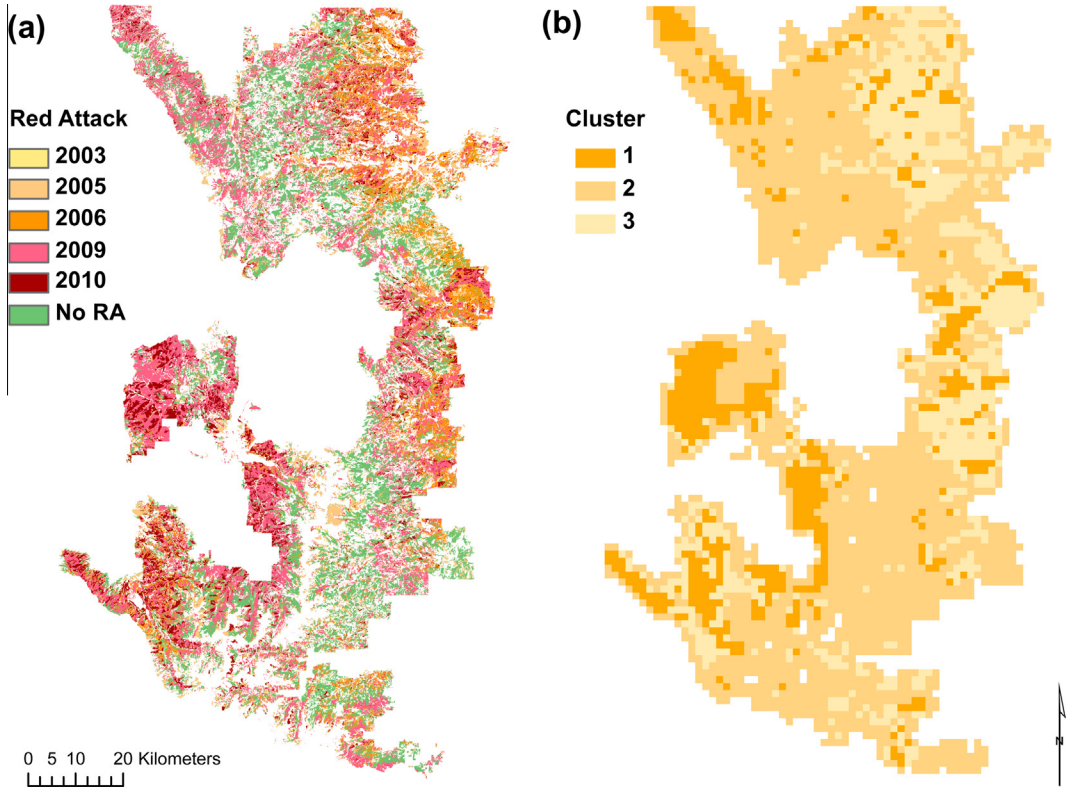

Fig. 2. (a) Results of change detection, demonstrating spread of MPB outbreak through time, and (b) Results of cluster analysis at 49 × 49 pixel scale. Results at this scale are not qualitatively different from the 25 × 25 and 99 × 99 scale. Grid cells in cluster 1showed red attack peaking early in the time series. In cluster 2, red attack peaked later in the outbreak, while cells in cluster 3 experienced little outbreak in any year. Grid cells where no outbreak was detected were removed from the analysis.

3. Results

3.1. Detection of red attack

Detection of red attack showed that MPB spread throughout the time series, with considerable mortality detected in 2005, 2006, and 2009 (Fig. 2). We detected 219 km^2 of red attack in 2003 (4% of forest in ARNF), 806 km^2 in 2005 (15%), 1874 km^2 in 2006 (35.4%), 1976 km^2 in 2009 (37%), and 416 km^2 in 2010 (8%). In total, red attack was detected in at least 1 year in 3216 km^2, 61% of forest in ARNF. Our method of discriminating between MPB-infested and uninfested areas performed well in 2003, 2005, and 2006 (Table 1). The quantity disagreement and allocation disagreement metrics partition misclassification into errors due to assigning the incorrect number of pixels to each class and to assigning those values to the incorrect location, respectively. For example in 2003 there was a 3% disagreement in the quantity of pixels assigned to each class and an 8% disagreement in the spatial allocation of those observations. In all years, misclassified pixels tended to be in stands with low canopy closure where a significant soil signature may contribute to confusion between the two classes.

Note that different areas were validated in different time steps (Fig. 1) because the extent of available high-resolution imagery was not sufficient to conduct an exhaustive validation at each time step. Consequently, we were unable to conclude whether or not our model performed better in one time step or another. Instead, we use our validation to demonstrate that our classification method had generally high accuracy and suggest that it provided data at sufficiently high resolution and accuracy to observe meaningful patterns in outbreak spatiotemporal development and to explore how MPB spread is related to environmental variables.

3.2. Outbreak spatiotemporal development

For each of three block sizes tested (25×25, 49×49 and 99×99 pixels), the optimal number of k clusters was 3. Similarly, visual comparison of these three block sizes showed that cluster pattern and identity were overwhelmingly similar regardless of scale, indicating that the results of time series cluster analysis were not scale dependent. Because all three scales were so similar, we describe only the patterns from the 49×49 block size (Fig. 2). In all clusters, proportion of mortality tended to be low in 2003. In cluster 1, mortality increased in 2005 and peaked in 2006 before declining in 2009 and 2010. In cluster 2 mortality peaks in 2009. Cluster 3 had generally low mortality throughout the time series. Areas having no pixels classified as red attack were not included in the analysis. Cells in cluster 1 occurred in several clumps around the study area, and many but not all cells in cluster 2 were near cells in cluster 1. Neither a distinct bulls-eye nor checkerboard pattern was present.

3.3. Conditional inference tree modeling

The 2003 CI tree had a misclassification rate of 5.8% and the area under the ROC curve (AUC) was 0.749. The CI tree classified sites at elevation >3340 m and having tree cover $\leqslant$65% as red attack, and red attack also occurred at well over the background rate of 5.8% at sites with southern (SE, S, SW) aspects that were above 3040 m. In the CI trees, sites are classified as red attack when >50% of observations in a terminal node were determined to represent red attack using remote sensing (Fig. 3). We used random forests to compute variable importance values for all variables included in the model. In addition to elevation, aspect, and percent tree cover, percent cover by lodgepole pine and percent cover by ponderosa pine were significant predictors of red attack occurrence (Fig. 4). Distance from nearest previous outbreak and area of nearest outbreak could not be calculated for this time step because it is the first year for which we were able to detect red attack.

Beginning with the 2005 CI tree, we added two spatial variables to account for beetle pressure, distance from nearest outbreak in the previous time step and area of nearest outbreak in the previous time step. The 2005 model had a misclassification rate of 16.5% and the area under the ROC curve was 0.669. Here, sites with tree cover <40% and elevation <2540 m were classified as red attack (Fig. 5). All sites with tree cover <55% experienced rates of red attack higher than the background rate of 14.9%. In this time step, random forests only identified tree cover and distance from 2003 outbreak as significant predictors.

The 2006 CI tree misclassified a 21.2% of observations model but its AUC (0.778) indicates the best performance, owing to improved discrimination between red attack and non-red attack classes. Sites were classified as red attack in 2006 if they were <2470 m in elevation, and those sites that were within 140 m of previous outbreak and had >55% cover by lodgepole pine experienced red attack at above the background rate of 22% (Fig. 6). In this time step, distance from 2005 outbreak, elevation, and% tree cover had significant variable importance values (Fig. 4).

For 2009, the CI tree misclassified 20.6% of observations and the AUC was 0.624. In this time-step, the rate of red attack in sites having >30% cover by lodgepole pine was above the background rate, but none were classified as red attack (training class: $n = 954$ observations, validation class: $n = 238$ observations, $p < 0.01$). Distance from 2006 outbreak, percentage of lodgepole pine, elevation,

Table 1
Validation of classification method represented by confusion matrices for (a) 2003, (b) 2005, and (c) 2006. Percentages in parenthesis indicate producer's accuracy for that class.

	Ground-truth			
	RA	Non-RA	Total	
(a) 2003				
Classified				
RA	7 (46.7%)	13	20	Allocation dis.: 8%
Non-RA	8	172 (93%)	180	Quantity dis.: 3%
Total	15	185	200 (89.5%)	
(b) 2005				
Classified				
RA	14 (70%)	13	27	Allocation dis.: 6%
Non-RA	6	167 (93.3%)	173	Quantity dis.: 4%
Total	20	180	200 (90.5%)	
(c) 2006				
Classified				
RA	104 (83%)	10	114	Allocation dis.: 10%
Non-RA	21	65 (86.7%)	86	Quantity dis.: 6%
Total	125	75	200 (84.5%)	

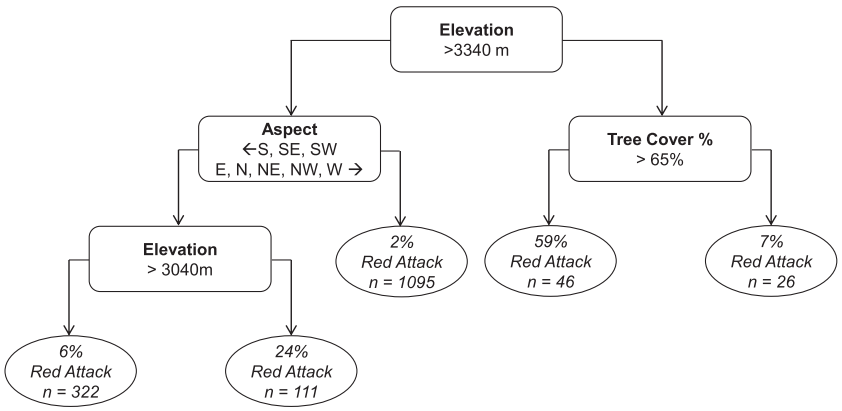

Fig. 3. Conditional inference tree model for 2003. Training class: $n = 1600$ observations, validation class: $n = 400$, misclassification rate = 5.75%, AUC = 0.749. All splits are statistically significant at the $p < 0.05$ level.

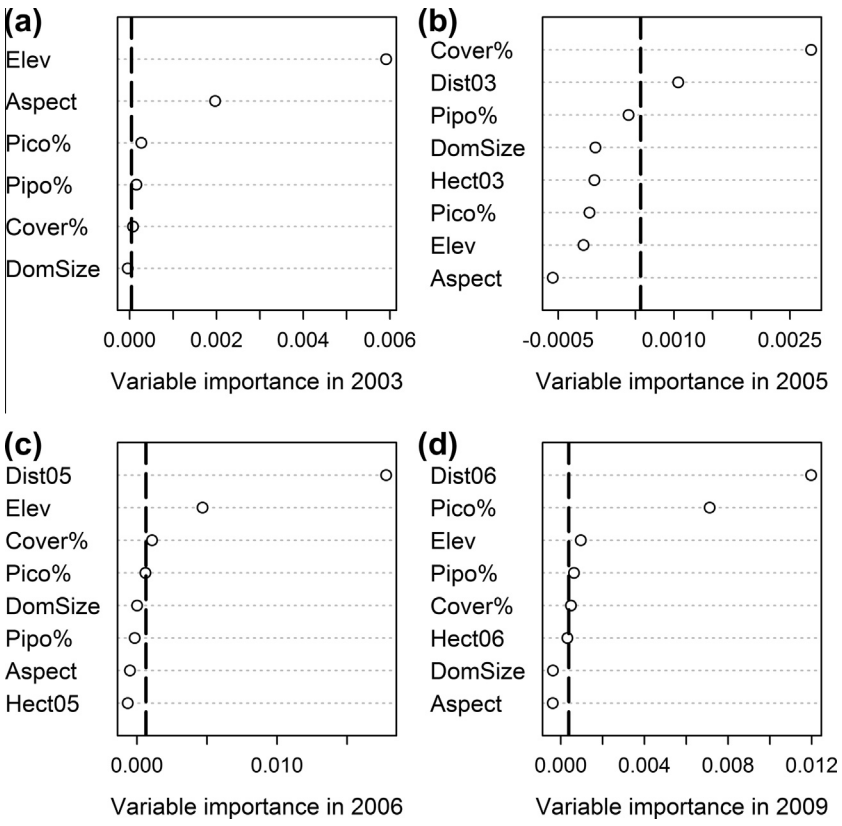

Fig. 4. Results of variable importance analysis using conditional forests for (a) 2003, (b) 2005, (c) 2006, and (d) 2009. Variables to the right of the dashed line are statistically significant predictors of MPB red attack occurrence.

percent cover by ponderosa pine and tree cover percent had significant variable importance values (Fig. 4).

4. Discussion

This study appeared to capture the spread of MPB red attack in Arapaho and Roosevelt National Forests from a period near the beginning of the outbreak through its crash; area of red attack was low in 2003, increased in 2005, peaked in 2006 and 2009, and declined sharply in 2010. We identified 4% of the study area as red attack in 2003, indicative of an ongoing landscape-level transition between the incipient-epidemic and epidemic population phases. Because at the incipient-epidemic phase MPB infests primarily small groups of trees (Safranyik and Carroll, 2006), much of the red attack at this stage may be undetected using 30 m resolution satellite images. USDA Forest Service Aerial Detection Survey maps (USDA Forest Service, 2013) confirm that MPB damage was relatively low in ARNF between 2000 and 2003, but our detection method may underestimate the total area of red attack in 2003 because a severe drought in summer 2002 likely depressed NDMI values. At the end of the time series, the amount of new red attack detected in 2010 was very low, signaling a population crash and the end of the outbreak cycle in the study area. Outbreaks can end due to a combination of unseasonably cold temperatures between late fall and early spring, and when the availability of host trees can no longer support high population sizes (Safranyik and Carroll, 2006).

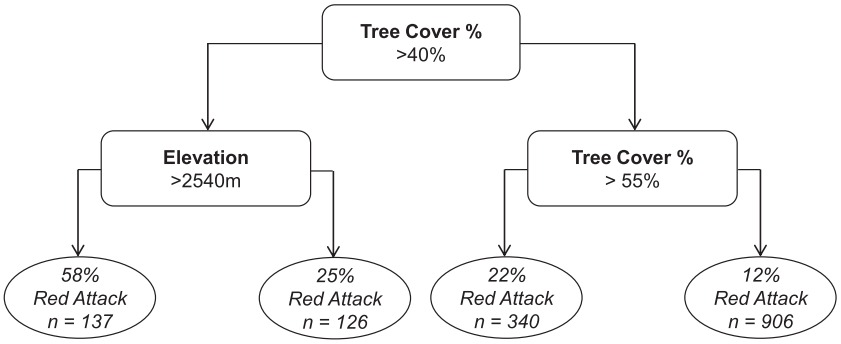

Fig. 5. Conditional inference tree model for 2005. Training class: $n = 1509$ observations, validation class: $n = 377$, misclassification rate = 16.45%, AUC = 0.669. All splits are statistically significant at the $p < 0.01$ level.

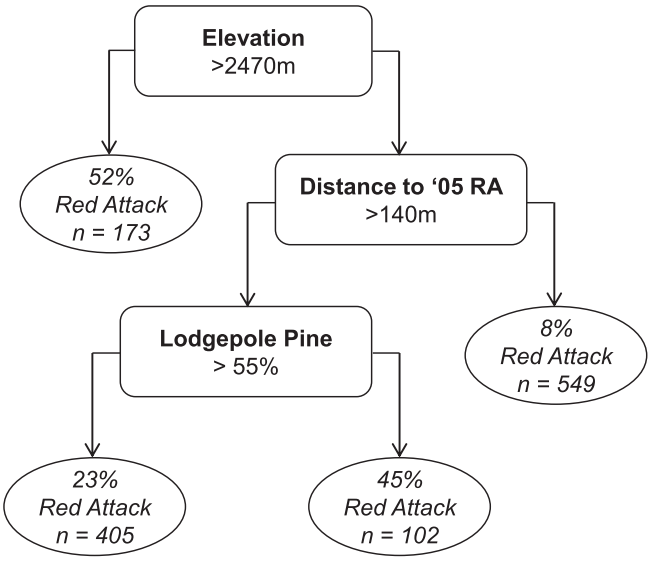

Fig. 6. Conditional inference tree model for 2006. Training class: $n = 1229$ observations, validation class: $n = 307$, misclassification rate = 21.17%, AUC = 0.778. All splits are statistically significant at the $p < 0.01$ level.

During the outbreak cycle, patterns of MPB spread were likely determined by both local habitat characteristics and dispersal between populations. In the cluster analysis, a bulls-eye pattern would be expected if dispersal and not local population growth were the dominant cause of a new infestation, whereas if the landscape consisted of many largely independent populations a checkerboard pattern would result. We detected a spatial pattern between these two extremes, which contrasts the pattern found by Aukema et al. (2006), who applied cluster analysis to a time series of MPB outbreak in British Columbia, Canada. In that study, a bulls-eye pattern suggested that the outbreak began with an epicenter in west-central British Columbia and radiated outward. Aukema et al. (2006), however, analyzed a $\approx 100\times$ larger area using a much coarser grain ($>4\times$ the largest block size in this study). Hence, differences between the two studies may be due to scale dependence.

Changes in the behavior of systems across spatial scales tend to occur abruptly and non-linearly (Wiens, 1989), so the lack of scale dependence at the spatial grains and extent covered in this study may not be indicative of patterns occurring over broader range of spatial scales. The differences between this and the Aukema et al. (2006) study could indicate a hierarchy of scales, where at coarse scales MPB outbreak spreads from an epicenter, but at fine scales its distribution is more strongly related to local environmental conditions. The differences observed between this and the Aukema study could also reflect characteristics of the two landscapes studied. In British Columbia, climate change has allowed MPB outbreaks to occur over areas that historically did not support them (Carroll et al., 2004). As it expanded its range, MPB populations in these areas may have been particularly sparse at the onset of the outbreak cycle, making them relatively more dependent on dispersal from epidemic populations than those in Colorado.

As suggested by spatiotemporal patterns of outbreak development, occurrence of red attack was associated with a combination of spatial relationships and environmental covariates. In this study, MPB infestation was associated with elevation, aspect, tree cover, species composition, and distance from an outbreak in a previous time step. A variable was considered associated with MPB infestation if it was included in a CI tree or had a significant variable importance value in at least 1 year. A key finding of this study is that, as an outbreak progresses, different variables best predict the occurrence of an infestation. Because most previous studies of susceptibility to MPB infestation have not taken a multi-temporal approach, the authors are not aware that this phenomenon has been previously demonstrated. Early in the outbreak cycle, a combination of environmental characteristics that accords well with previous research on susceptibility to MPB infestations were the best predictors of red attack (Fig. 3). As the outbreak progressed, distance from a detected infestation in the previous time step, a measure of beetle pressure (Shore and Safranyik, 1992), increased in importance relative to other predictors (Fig. 4), while the environmental characteristics associated with red attack also changed (Figs. 5 and 6). At the end of the outbreak, red attack was primarily associated with stands with high abundance of host trees, suggesting that the outbreak declined when the availability of host trees failed to support its population levels.

The year 2003 represents a landscape where stands are transitioning between the incipient-epidemic and epidemic population phases. During this period, variables related to susceptibility should be good predictors of red attack because MPB populations are either still dependent on susceptible trees or were recently and show the spatial signature of the susceptible areas where the outbreak originated. We found rates of red attack in 2003 to be associated with high elevation, southern aspects, moderately high tree cover, and the percent cover of lodgepole and ponderosa pine. Dense stands of major hosts may be susceptible to infestation because competition reduces tree vigor (Larsson et al., 1983), and susceptibility may increase on south-facing slopes because higher levels of solar radiation may increase tree stress and beetle survival (Coops et al., 2006).

The areas of red attack detected in 2005, 2006, 2009 represent growth and peak within the outbreak phase at the landscape level. Throughout this period, the distance from the nearest outbreak in

the previous time step was a significant predictor of spread, including the most significant in 2006 and 2009 (Fig. 4). As more of the landscape reaches the epidemic phase, beetle pressure should become the most important determinant of new infestations because populations are sufficiently large to overcome the defenses of healthy trees via mass attack (Mitchell and Preisler, 1991; Logan et al., 1998). Measures of beetle pressure typically include an approximation of population size based on numbers of infested trees (Shore and Safranyik, 1992), but in this study a related metric, area of nearest outbreak in the previous time step, was not an important variable in any year (Fig. 4). Our measures of beetle pressure could not be calculated for 2003, but we expect it to have relatively low importance based on known patterns of outbreak development (Mitchell and Preisler, 1991; Logan et al., 1998), the trajectory of its change in importance between 2005 and 2009, and the relative importance of environmental covariates in 2003.

At the same time as beetle pressure became a dominant influence on the landscape, the environmental characteristics of new red attack sites also changed. Rates of red attack were high at sites with relatively high percent tree cover in 2003 and lower percent tree cover in 2005, and the variable's importance declined after 2005. Susceptibility to MPB can increase with forest density because competition reduces tree vigor (Larsson et al., 1983), so, taking forest cover as a proxy for density, red attack appeared to occur in more susceptible stands at the onset of the outbreak, but after reaching the epidemic level moved to less dense stands where trees may have been more vigorous and thus provided more nutrition. Though the density of trees became less important in the second half of the outbreak cycle, host tree abundance appeared to influence which sites became infested late in the outbreak (Figs 5 and 6). Suitable host trees may be depleted in sites where pine species, particularly lodgepole pine, the primary host for MPB, are not abundant. Percent ponderosa pine, a major MPB host tree, did not appear in any CI trees, but was a significant predictor in 2003 and 2009, years when forest composition may be particularly important.

From the beginning of the study period through the outbreak crash, areas of new infestation were also characterized by different elevations. Red attack moved from high elevations to in 2003 to low elevations in 2005 and 2006, which may clarify conflicting findings regarding the relationship between red attack presence and elevation (Coops et al., 2006; White et al., 2006; Wulder et al., 2006a). At the beginning of recent MPB outbreaks in British Columbia, Canada, infestation hot spots developed near the elevation limit for MPB to maintain univoltine life cycles (Nelson et al., 2007). In this study, red attack was detected in 2003 at elevations that Amman (1973) found to be above the limit of MPB for the range of latitudes represented in ARNF, although recent research suggests that MPB outbreaks have historically occurred at elevations >3000 m (J.F. Negrón personal communication). Decades of climate warming have also enhanced the suitability of high latitudes and elevations to MPB (Carroll et al., 2004; Bentz et al., 2010).

Despite the strong relationship between tree diameter and brood production (Amman, 1972; Safranyik et al., 1974), size class was neither included in the CI tree nor had a significant variable importance value in any year. We do not, however, conclude that tree size was unimportant to MPB population dynamics in ARNF during our study. Size class in the R2Veg database describes the size of the dominant trees in a stand by binning it into five classes, so the width of the bins and the spatial grain of the data may not be precise enough to use size class to predict red attack. This result highlights the importance of developing models based on data readily available to forest managers.

While the identity of significant predictors of red attack changed over the study period, the ability of the CI trees to discriminate between infested and uninfested areas also varied. The CI tree for 2009 was the weakest at discriminating between the red attack and non-red attack classes. The CI tree for 2005 also performed less well than 2003 and 2006, suggesting that to the longer time interval between change detection images (2 and 3 years, versus 1 year) could result in poor performance. Given that predictors of MPB infestation appear to change as an outbreak cycle progresses, it would be more difficult to predict the results of 2 or 3 years of MPB activity than a single year. The explanatory power of the CI trees could also decline if a longer time interval also increases the amount of uncertainty in estimates of outbreak location and extent based on remotely sensed imagery. In practice, we have no evidence that the change detection methods employed in this study perform less well when the time interval between images increases. In all 3 years we were able to validate, total accuracy was $\geqslant$ 84.5% and the lowest accuracy occurred in 2006, a 1 year time step. These accuracies are comparable to other studies using Landsat imagery, which report accuracies between 70% and 86% (Coops et al., 2006; Wulder et al., 2006a; Goodwin et al., 2008). Though we were unable to validate the 2009 red attack map, the strong performance of our classification methods in three other time steps suggests that our methods continued to identify red attack with good accuracy.

Despite some uncertainty over the accuracy of the 2009 red attack map, an ecological explanation for having the lowest CI tree performance in that year should not be discounted. Nelson et al. (2007) found that during a recent outbreak in British Columbia highly susceptible stands were attacked early in the outbreak cycle and as the outbreak progressed the characteristics of infested stands approached the background distribution and thus would be difficult to distinguish from un-infested stands using environmental covariates. Because we have a small number of time steps and the lengths vary due to gaps in the availability of suitable Landsat imagery, confidence in this result is tempered, but if this pattern could be found in other areas it would underscore the importance of early management interventions, when the spread of MPB is more predictable.

One important question is whether the patterns found in this study would apply to other landscapes. While our findings are unique, they do fit within scientific understanding of mountain pine beetle epidemiology and tree and stand-level susceptibility to infestation (Fettig et al., 2007). Still, other outbreaks might deviate from the patterns we found for several reasons. The elevations having thermal conditions favorable to MPB are tied to latitude, so caution should be taken when extrapolating those values to other locations even though there is some evidence that infestations early in outbreaks occur near the limit of MPB's elevation range (Nelson et al., 2007). Species composition may be important late in the outbreak primarily when it crashes due to a lack of available host trees; when weather fluctuations are strong the outbreak could crash before host unavailability is felt strongly. Additionally, the variables available in the R2Veg database were not a one-to-one match to those measured in other studies and may not match similar forest inventories for other areas.

Recent works have prescribed managing against MPB outbreaks by combining long-term strategies to reduce the susceptibility of stands and landscapes with activities that identify growing populations and reduce their numbers (Shore et al., 2006). Our findings support the use of such an approach; spread of MPB outbreak was attributed to a combination of stand susceptibility and beetle pressure. We also found that the best covariates for predicting red attack changed over the course of the outbreak. If this pattern is consistent it could help forest managers by allowing risk estimates to be specific to the point in the outbreak cycle, which could be especially helpful in the epidemic population phase when new red attack is produced from a combination of dispersal and

within-stand population growth. Future research could address whether the spatiotemporal development of MPB outbreaks at other times and places is similar to what we have observed.

5. Conclusions

Mountain pine beetle infestation has dramatically impacted Arapaho–Roosevelt National Forest. Our findings suggest a cycle where severe MPB outbreak began in the early 2000s, spread throughout the decade, and has declined toward endemic population levels. By building explanatory models of MPB spread throughout the outbreak, we have identified that the factors associated with incidence of red attack change during the outbreak cycle. Our findings demonstrate a general pattern where, from outbreak inception to crash, the major controls on the spread of the infestation change from forest susceptibility to dispersal to host availability. At the beginning of the time series, when stands were transitioning between the incipient-epidemic and epidemic population phases, topography and stand structure variables associated with susceptibility to MPB infestation had high weight as predictors of red attack. The outbreak developed further in subsequent years and beetle pressure became increasingly important to spread of the infestation, but the elevation, forest density, and species composition of newly attacked sites also changed as the outbreak developed, with abundance of major hosts lodgepole and ponderosa pine growing in importance at the end of the study period. Though these findings fit solidly within the known ecology of MPB populations, highlighting this pattern opens up new lines of inquiry and can aid in targeting management interventions against mountain pine beetle outbreaks.

Acknowledgements

The authors would like to thank Kyle Haynes, Jill Greiner, the Terrestrial Ecology group at the University of Virginia, José F. Negrón and an anonymous reviewer for comments that improved the manuscript. We would also like to thank Gettysburg College, the University of Virginia Department of Environmental Sciences and Blandy Experimental Farm for their support.

References

Amman, G.D., 1972. Mountain pine beetle brood production in relation to thickness of lodgepole pine phloem. J. Econ. Entomol. 65 (1), 138–140.
Amman, G.D., 1973. Population changes of the mountain pine beetle in relation to elevation. Environ. Entomol. 2, 541–547.
Aukema, B.H., Carroll, A.L., Zhu, J., Raffa, K.F., Sickley, T.A., Taylor, S.W., 2006. Landscape level analysis of mountain pine beetle in British Columbia, Canada: spatiotemporal development and spatial synchrony within the present outbreak. Ecography 29 (3), 427–441.
Bentz, B.J., Régnière, J., Fettig, C.J., Hansen, E.M., Hayes, J.L., Hicke, J.A., Kelsey, R.G., Negrón, J.F., Seybold, S.J., 2010. Climate change and bark beetles of the western United States and Canada: direct and indirect effects. Bioscience 60, 602–613.
Carroll, A.L. Taylor, S.W., Régnière, J., Safranyik, L., 2004. Effects of climate change on range expansion by the mountain pine beetle in British Columbia. In: Shore, T.L., Brooks, J.E., Stone, J.E. (Eds.), Mountain Pine Beetle Symposium: Challenges and Solutions, 30–31 October 2003, Kelowna, British Columbia, Canada. Natural Resources Canada, Canadian Forest Service, Pacific Forestry Centre, Victoria, British Columbia, Information, Report BC-X-399, pp. 223–232.
Chander, G.B., Markham, B., 2003. Revised Landsat-5 TM radiometric calibration procedures and postcalibration dynamic ranges. IEEE Trans. Geosci. Remote Sens. 41, 2674–2677.
Chander, G.B., Markham, B., Helder, D., 2009. Summary of current radiometric calibration coefficients for Landsat MSS, TM, ETM+, and EO-1 ALI Sensors. Remote Sens. Environ. 113, 893–903.
Coops, N.C., Wulder, M.A., White, J.C., 2006. Integrating remotely sensed and ancillary data sources to characterize a mountain pine beetle infestation. Remote Sens. Environ. 105, 83–97.
De'ath, G., Fabricius, K.E., 2000. Classification and regression trees: a powerful yet simple technique for ecological data analysis. Ecology 81, 3178–3192.
Dillman, R.D., White, W.B., 1982. Estimating mountain pine beetle-killed ponderosa pine over the front range of Colorado with high altitude panoramic photography. Photogramm. Eng. Remote Sens. 48, 741–747.
Fettig, C.J., Klepzig, K.D., Billings, R.F., Munson, A.S., Nebeker, T.E., Negón, J.F., Nowak, J.T., 2007. The effectiveness of vegetation management practices for prevention and control of bark beetle infestations in coniferous forests of the western and southern United States. For. Ecol. Manage. 238, 24–53.
Fielding, A.H., Bell, J.F., 1997. A review of methods for the assessment of prediction errors in conservation presence/absence models. Environ. Conserv. 24, 38–49.
Goodwin, N.R., Coops, N.C., Wulder, M.A., Gillanders, S., Schroeder, T.A., Nelson, T., 2008. Estimation of insect infestation dynamics using a temporal sequence of Landsat data. Remote Sens. Environ. 112, 3680–3689.
Hothorn, T., Hornik, K., Zeileis, A., 2006. Unbiased recursive partitioning: a conditional inference framework. J. Comput. Graph. Sci. 15, 574–651.
Jenkins, M.J., Hebertson, E., Page, W., Jorgensen, C.A., 2008. Bark beetles, fuels, fires and implications for forest management in the Intermountain West. For. Ecol. Manage. 254, 16–34.
Jenkins, M.J., Page, W.G., Hebertson, E.G., Alexander, M.E., 2012. Fuels and fire behavior dynamics in bark beetle-attacked forests in Western North America and implications for fire management. For. Ecol. Manage. 275, 23–34.
Jin, S., Sader, S.A., 2005. Comparison if time series tasseled cap wetness and the normalized difference moisture index in detecting forest disturbances. Remote Sens. Environ. 94, 364–372.
Jolly, W.M., Parsons, R.A., Hadlow, A.M., Cohn, G.M., McAllister, S.S., Popp, J.B., Hubbard, R.M., Negrón, J.F., 2012. Relationships between moisture, chemistry, and ignition of *Pinus contorta* needles during the early stages of mountain pine beetle attack. For. Ecol. Manage. 269, 52–59.
Klein, W.H., 1982. Estimating bark beetle-killed lodgepole pine with high-altitude panoramic photography. Photogramm. Eng. Remote Sens. 48, 733–737.
Klutsch, J.G., Battaglia, M.A., West, D.R., Costello, S.L., Negrón, J.F., 2011. Evaluating potential fire behavior in lodgepole pine-dominated forests after a mountain pine beetle epidemic in north-central Colorado. Western J. Appl. For. 26, 101–109.
Landsat 7 Science Data Users Handbook, 2007. NASA Goddard Space Flight Center. <http://landsathandbook.gsfc.nasa.gov/handbook> (accessed 03.13).
Larsson, S., Oren, R., Waring, R.H., Barrett, J.W., 1983. Attacks of mountain pine beetle as related to tree vigor of ponderosa pine. For Sci. 29 (2), 395–402.
Liebhold, A.M., Elkinton, J.S., 1989. Characterizing spatial patterns of gypsy moth regional defoliation. For. Sci. 35 (2), 557–568.
Logan, J.A., White, P., Bentz, B.J., Powell, J.A., 1998. Model analysis of spatial patterns in mountain pine beetle outbreaks. Theor. Popul. Biol. 53, 236–255.
MacQueen, J.B., 1967. Some methods for classification and analysis of multivariate observations. In: Proceedings of 5th Berkeley Symposium on Mathematical Statistics and Probability, University of California Press, pp. 281–297.
Marr, J.W., 1961. Ecosystems of the east slope of the Front Range in Colorado. University of Colorado Studies Series in Biology 8. University of Colorado Press, Boulder, CO.
Meddens, A.J.H., Hicke, J.A., Vierling, L.A., 2011. Evaluating the potential of multispectral imagery to map multiple stages of tree mortality. Remote Sens. Environ. 115, 1632–1642.
Mitchell, R.G., Preisler, H.K., 1991. Analysis of spatial patterns of lodgepole pine attacked by outbreak populations of the mountain pine beetle. For. Sci. 37 (5), 1390–1408.
Nelson, T.A., Boots, B., Wulder, M.A., Carroll, A.L., 2007. Environmental characteristics of mountain pine beetle infestation hot spots. BC J. Ecosyst. Manage. 8 (1), 91–108.
Peet, R.K., 1981. Forest vegetation of the Colorado front range: composition and dynamics. Vegetatio 45, 3–75.
Pontius Jr., R.G., Millones, M., 2011. Death to Kappa: birth of quantity disagreement and allocation disagreement for accuracy assessment. Int. J. Remote Sens. 32 (15), 4407–4429.
R Core Team, 2012. R: A language and environment for statistical computing. R Foundation for Statistical Computing, Vienna, Austria <http://www.R-project.org/>.
Safranyik, L., Carroll, A.L., 2006. The biology and epidemiology of the mountain pine beetle in lodgepole pine forests. In: Safranyik, L., Wilson, B. (Eds.), The Mountain Pine Beetle: A Synthesis of Biology, Management, and Impacts on Lodgepole Pine. Canadian Forest Service, Victoria, British Columbia, Canada, pp. 3–66.
Safranyik, L., Shrimpton, D.M., Whitney, H.S., 1974. Management of lodgepole pine to reduce losses from the mountain pine beetle. Environment Canada, Canadian Forestry Service, Pacific Forest Research Centre, Victoria, BC. Forestry Technical, Report 1.
Schoennagel, T., Veblen, T.T., Negron, J.F., Smith, J.M., 2012. Effects of mountain pine beetle on fuels and expected fire behavior in lodgepole pine forests, Colorado, USA. PLoS ONE 7, e30002.
Shore, T.L., Safranyik, L., 1992. Susceptibility and risk rating systems for the mountain pine beetle in lodgepole pine stands. Forestry Canada Information, Report BC-X-336.
Shore, T.L., Safranyik, L., Lemieux, J.P., 2000. Susceptibility of lodgepole pine stands to the mountain pine beetle: testing of a rating system. Can. J. For. Res. 30, 44–49.
Shore, T.L., Safranyik, L., Whitehead, R.J., 2006. Principles and concepts of management. In: Safranyik, L., Wilson, B. (Eds.), The Mountain Pine Beetle: A Synthesis of Biology, Management, and Impacts on Lodgepole Pine. Canadian Forest Service, Victoria, British Columbia, Canada, pp. 117–121.

Simard, M., Romme, W.H., Griffin, J.M., Turner, M.G., 2011. Do mountain pine beetle outbreaks change the probability of active crown fire in lodgepole pine forests? Ecol. Monogr. 81, 3–24.
Sims, C., Aadland, D., Finoff, D., 2010. A dynamic bioeconomic analysis of mountain pine beetle epidemics. J. Econ. Dynam. Control 34, 2407–2419.
Sing, T., Sander, O., Beerenwinkel, N., Lengauer, T., 2005. ROCR: visualizing classifier performance in R. Bioinformatics 21, 3940–3941.
Song, C., Woodcock, C.E., Seto, K.C., Lenney, M.P., Macomber, S.A., 2001. Classification and change detection using Landsat TM data: when and how to correct atmospheric effects? Remote Sens. Environ. 75, 230–244.
Strobl, C., Boulesteix, A.L., Kneib, T., Augustin, T., Zeileis, A., 2008. Conditional variable importance for random forests. BMC Bioinformatics 9. http://dx.doi.org/10.1186/1471-2105-9-307.
Strobl, C., Tutz, G., Malley, J., 2009. An introduction to recursive partitioning: rationale, application, and characteristics of classification and regression trees, bagging, and random forests. Psychol. Method 14, 323–348.
Taylor, S.W., Carroll, A.L., 2004. Disturbance, forest age, and mountain pine beetle outbreak dynamics in BC: a historical perspective. In: Shore, T.L., Brooks, J.W., Stone, J.E. (Eds.), Mountain Pine Beetle Symposium: Challenges and Solutions, Kelowna, British Columbia, Canada. Natural Resources Canada, Canadian Forest Service, Pacific Forestry Centre, Victoria, British Columbia, Information, Report BC-X-399, October 2003, pp. 30–31 (pages 41–51).
USDA Forest Service, 2009. R2veg. Online. <http://www.mpcer.nau.edu/sage/SJPLC/r2veg.htm#6> (accessed 12.03.13).
USDA Forest Service, 2012. Forest Health Management. Online. <http://fs.usda.gov/main/barkbeetle/barkbeetlemanagement/foresthealthmanagement> (accessed 15.03.13).
USDA Forest Service, 2013. Aerial Detection Survey: Data Download. Online <http://www.fs.usda.gov/detail/r2/forest-grasslandhealth> (accessed 15.03.13).
Westfall, J., 2007. 2006 Summary of forest health conditions in British Columbia. Ministry of Forests, Forest Practices Branch, Victoria, BC.
Wiens, J.A., 1989. Spatial scaling in ecology. Funct. Ecol. 3, 297–385.
Williams, D.W., Liebhold, A.M., 2000. Spatial synchrony of spruce budworm outbreaks in eastern North America. Ecology 81 (10), 2753–2766.
White, J.C., Wulder, M.A., Grills, D., 2006. Detection and mapping mountain pine beetle red-attack damage with SPOT-5 10-m multispectral imagery. BC J. Ecosyst. Manage. 7, 105–118.
Wulder, M.A., White, J.C., Bentz, B., Alvarez, M.F., Coops, N.C., 2006a. Estimating the probability of mountain pine beetle red attack damage. Remote Sens. Environ. 101, 150–155.
Wulder, M.A., Dymond, C.C., White, J.C., Erickson, B., 2006b. Detection, mapping, and monitoring of the mountain pine beetle. In: Safranyik, L., Wilson, B. (Eds.), The Mountain Pine Beetle: A Synthesis of Biology, Management, and Impacts on Lodgepole Pine. Canadian Forest Service, Victoria, British Columbia, Canada, pp. 123–154.